# Spectroscopic Studies of Pyridine-Containing Polyurethanes Blended with Metal Acetates

**Ellen M. O'Connell,[†] Chang-Zheng Yang,[‡] Thatcher W. Root, and Stuart L. Cooper*[,§]**

*Department of Chemical Engineering, University of Wisconsin−Madison, Madison, Wisconsin 53706*

*Received September 26, 1995; Revised Manuscript Received June 5, 1996*[⊗]

ABSTRACT: Natural-abundance $^{15}N$ nuclear magnetic resonance (NMR) experiments show direct evidence for metal−pyridine interactions in blends of pyridine-containing polyurethanes and metal acetates. After blending with zinc acetate, the pyridine nitrogen peak shifts from −320 to −304 ppm; blending with magnesium acetate causes a shift to −309 ppm. Sodium acetate did not complex with the pyridine-containing polyurethanes; no shifts in the $^{13}C$ NMR signal for the acetate carbonyl or in the $^{15}N$ NMR for the pyridine nitrogen are apparent. Additionally, no interactions were evident for the urethane nitrogen site in any of the blends. Peak shifts, changes in cross-polarization dynamics, and increases in relaxation times were also apparent in the $^{13}C$ NMR spectra of the metal acetate−polymer blends. Effects of blending on the hard-domain hydrogen bonding were evident in FTIR and $^{15}N$ NMR contact-time experiments. The N−H stretching band shifted to higher wavenumbers and the $^{15}N$ NMR N−H signal persisted to longer contact times for the blend. Both spectroscopic techniques give evidence for complexation in these polyurethane blends.

## Introduction

Polyurethanes are linear block copolymers that are classified as thermoplastic elastomers. These copolymers are phase-separated materials in which one phase consists of rubbery or "soft" domains and the other glassy or semicrystalline "hard" domains. The microphase separation is caused by the incompatibility of the hard and soft segments, with the hard domains acting as physical cross-links and reinforcing filler.

Recently, researchers have studied blends of polymers, including thermoplastic elastomers, containing complexing agents. One of the most commonly used polymers for complexation is poly(4-vinylpyridine) (P4VP), or poly(styrene-*co*-4-vinylpyridine) (PSVP), because the pyridine nitrogen is believed to coordinate readily with transition metal ions. Agnew[1] first presented evidence of interactions in blends of metal chlorides with vinylpyridines and P4VP. Meyer and Pineri[2−5] demonstrated iron complexation with iron chloride blended in a terpolymer of butadiene, styrene, and P4VP using Mössbauer spectroscopy, SAXS, and electron microscopy. Peiffer *et al.*[6,7] showed interaction in blends of a zinc-neutralized sulfonated thermoplastic elastomer (Zn-S-EPDM) and PSVP. Blending the interacting components led to marked improvements in tensile properties, melt viscosity, and dynamic mechanical properties compared to a blend of Zn-S-EPDM and polystyrene. Their results suggested coordination in 1:1 stoichiometric blends for $Zn^{2+}$- and $Cu^{2+}$-neutralized blends. Strong interaction effects were present with transition metal ions, but not with sodium or magnesium ions. Therefore, for these systems the mode of interaction was described to be transition-metal complexation with the pyridine-nitrogen lone pair of electrons.

Lu and Weiss[8] studied the solution behavior of mixtures of neutralized sulfonated polystyrene ionomers and PSVP. They found interactions in blends with alkali and alkaline earth metals as well as with transition metals. The authors proposed a schematic of the intermolecular complex in which the cation is solvated by a relatively polar solvent, permitting coordination between the pyridine nitrogen and the sulfonate oxygen. It was suggested that the intermolecular complex for alkali or alkaline earth metal blends can be described by this solvated-ion scheme, which relies on the electrostatic fields of the cations for interaction. On the other hand, the formation of ion pairs is favored in transition-metal complexes, indicating a mechanism of metal−ligand coordination bonding.

Belfiore *et al.*[9] studied transition-metal complexes in ionomeric blends composed of either P2VP or P4VP and $Zn^{2+}$-neutralized ethylene−methacrylic acid (Zn-EMAA). When Zn-EMAA and P4VP are blended, a $^{13}C$ NMR peak appears near 180 ppm; this is attributed to carboxylic acid carbons near $Zn^{2+}$ ions, which complex with the pyridine nitrogen's lone pair of electrons. This peak is missing when P2VP is used in place of P4VP, suggesting that steric hindrance prevents complexation. The fact that the carbon resonances from the acid carbonyl (185 ppm) and the uncomplexed $Zn^{2+}$-neutralized carbonyl (189 ppm) are still seen suggests a phase-separated system. Mechanical data from tensile testing supported this conclusion.

In a continuation of this study, Belfiore *et al.*[10,11] reported transition-metal coordination in both model compounds and polymer blends. The authors looked at blends of P4VP and several zinc salts (acetate, laurate, and stearate).[11] $^{13}C$ NMR spectra of the carbonyl group in zinc acetate showed a shift from 185 (crystalline) to 179 ppm in blends containing 28 mol % zinc acetate. It was suggested that the peak shift was due to complexation with the pyridine nitrogen. Blends with zinc laurate and zinc stearate with P4VP showed peaks at both 181 and 185 ppm, indicating that both amorphous and crystalline phases of the zinc salt were present. No evidence for complexation was seen in blends with magnesium acetate. This was attributed to the pref-

* Author to whom correspondence should be addressed.
[†] Present address: Air Products and Chemicals, Inc., 7201 Hamilton Blvd., Allentown, PA 18195−1501.
[‡] Permanent address: Department of Chemistry, Nanjing University, Nanjing, People's Republic of China.
[§] Present address: College of Engineering, University of Delaware, Newark, DE 19716.
[⊗] Abstract published in *Advance ACS Abstracts,* August 1, 1996.

S0024-9297(95)01441-0 CCC: $12.00 

erential complexation of magnesium, a hard acid, to acetate or water instead of to the pyridine nitrogen, a weak base.

In two previous papers studying the effects of complexation in phase-separated polymers, we have described a new polyurethane containing a pendant pyridine group (Figures 1a,c).[12,13] Enhancements in tensile and dynamic mechanical properties were seen when these new materials were blended with transition-metal acetates; for example, the moduli of the blends were 10−35 times that of the precursor material.[12] The proposed morphology of a polyurethane containing 54 wt % hard-segment material (PU-35) was that of an interconnected hard domain, while a polyurethane with a lower hard-segment content (42 wt %, PU-29) possessed a dispersed hard-domain morphology, with the soft domain as the continuous phase. Addition of the metal acetates to PU-35 improved the hard-domain cohesion and strength dramatically but only slightly affected the phase separation. For PU-29, it was suggested that addition of the metal ions increased the number of physical cross-links, but again altered the phase separation only slightly. This was confirmed with small-angle X-ray scattering (SAXS) experiments.[13] The morphology of the material was not dramatically affected by the blending; the position of the SAXS peak did not shift appreciably with blending. EXAFS studies were undertaken to determine the local structure surrounding the cations in the blends, but results were inconclusive.[13]

This paper continues a molecular-level approach to understand the factors contributing to the improved properties of the blends. Since the hard-segment components appear to be the key to the behavior of the polyurethane, most discussion will be on PU-35 and hard-segment-only materials. $^{13}C$ NMR and $^{15}N$ NMR (at natural abundance) were used to study the carbon and nitrogen sites in the urethane linkage and the pyridine chain extender, as well as the carbon nuclei in the acetate complexing agent. Natural-abundance $^{15}N$ NMR studies are less common than investigations using enriched materials, but have been reported in the literature.[14,15] FTIR studies were undertaken to identify changes in the pyridine and urethane nitrogen regions with blending. The goal was to correlate the effects of blending to changes in the chemical shifts and relaxation times for the carbon and nitrogen sites on the pyridine group that are proposed to interact with the metal salts. The results can be used to explain the mechanical and morphological properties acquired from tensile testing and small-angle X-ray scattering. In this way, the structure−property relationships of the blends can be determined.

## Experimental Section

The polyurethanes were synthesized using a two-step reaction. The materials are based on 3/2/1 or 2/1/1 molar ratios of methylenebis(phenyl isocyanate) (MDI), *N,N*-bis(2-hydroxyethyl)isonicotinamide (BIN), and poly(tetramethylene oxide) (PTMO, MW = 1000). The complete synthesis procedure has been reported.[12] The polyurethanes (10 wt % in dimethylformamide (DMF)) were then blended with a stoichiometric amount of metal acetate (zinc, magnesium, or sodium) dissolved in DMF so that the molar ratio of pyridine to acetate was 1:1 for all blends. Following the sample identification given in the two previous papers, materials are identified as XX-##, where XX is PU for the base polyurethane or the metal cation ($Zn^{2+}$, $Mg^{2+}$, or $Na^{+}$) for the blends, and ## is the weight fraction of MDI units (29% for 2/1/1 and 35% for 3/2/1 mole ratios). All materials were dried to remove solvent but allowed to equilibrate in air before testing.

Isocyanate:chain extender 1:1 hard-segment-only materials were synthesized in a manner similar to that used for the polyurethanes. BIN was dissolved in anhydrous *N,N*-dimethylacetamide (DMAc) under a dry nitrogen gas purge and stirred constantly. The solution was heated to 60 °C and the catalyst (dibutyltin dilaurate) and the isocyanate (MDI, already dissolved in anhydrous DMAc) were added. The reaction was stirred for 1 h at 65 °C and then for 2−3 h at 80 °C. The polymer solution was allowed to cool to room temperature and then was precipitated in a large volume of water. The polyurethane product was soaked in water overnight, filtered, and dried in a convection oven at 60 °C for several hours, followed by drying in a vacuum oven at 60 °C for 1 week. The IR spectrum showed that all the isocyanate groups had been reacted with hydroxyl groups. The 1:1 MDI/butanediol (BD) hard-segment material was synthesized in an equivalent manner by R. J. Goddard at the University of Wisconsin using stannous octoate as the catalyst. Residual DMF was identified from an IR band at 1666 $cm^{-1}$, as $^{13}C$ NMR peaks at 31, 36, and 162 ppm, or as a $^{15}N$ NMR peak at −260 ppm. DMF could be removed by drying at 65 °C for ∼1 week for the polyurethanes containing soft segments and 80 °C for ∼3 weeks for the hard-segment-only materials. DMF, tetrahydrofuran (THF), DMAc, and BIN were acquired from Aldrich. PTMO was received from QO Chemicals, MDI from Polysciences, and the stannous octoate catalyst from Air Products.

Materials for uniaxial stress−strain experiments were cast from 5 wt % solutions of DMF onto Teflon dishes. Data were obtained on an Instron Model TM using a crosshead speed of 0.5 in./min. The Instron was interfaced to a personal computer for automatic data acquisition. Samples were cut with an ASTM D1708 die. Data are reported as engineering stress versus elongation and are the average of three or more tests.

Infrared spectra of the pyridine-containing polyurethanes were acquired using a Mattson Model GL-5020 spectrometer with a MCT detector. The resolution was 2 $cm^{-1}$ and the number of scans acquired varied from 16 to 64. Samples were cast from 1 wt % solutions of either THF or DMF directly onto KBr plates. The film thickness was controlled so that the absorbance of the material was less than 1, to stay within the range in which the Beer−Lambert law is valid.[16]

NMR spectra of the polyurethanes were acquired on a Chemagnetics CMC-300A spectrometer at 75.4 MHz for $^{13}C$ NMR and 30.3 MHz for $^{15}N$ NMR. $^{13}C$ NMR spectra were acquired in a 7.5 mm probe using zirconia rotors; magic angle spinning (typically 5 kHz), cross-polarization, and high-power proton decoupling were employed. The secondary reference was the methyl carbon of hexamethylbenzene, which is $\delta$ = 17.3 ppm from tetramethylsilane (TMS). $^{15}N$ NMR spectra were obtained using a 9.5 mm probe and Delrin rotors. Cross-polarization, high-power proton decoupling, and magic angle spinning (typically 2−3 kHz) were employed. The frequency axis was set using an external reference of glycine, which has a chemical shift $\delta = -350$ ppm relative to the standard $CH_3$-$NO_2$. Pulse delays of 5 s were used for all cross-polarized spectra.

$^{23}Na$ FTNMR spectra were acquired at 79.2 MHz. The frequency axis was set using an external reference of NaCl(s), which has a chemical shift $\delta$ = 7.1 ppm relative to the standard NaCl(aq) solution. All solid samples were run in zirconia rotors using magic angle spinning (typically 5 kHz) and high-power proton decoupling. To achieve uniform excitation, which permits quantitative analysis of the peak areas, the samples were run with a pulse width of 1.2 $\mu$s (corresponding to a 12.7° tip).[17,18]

## Results and Discussion

A schematic of the components of PU-35 and a poly(ether−urethane) is shown in Figure 1. The traditional polyurethane does not contain the pyridine group in the chain extender. Figure 2 shows the stress−strain curves of PU-35 and its blend with several transition-metal acetates. These curves are somewhat different

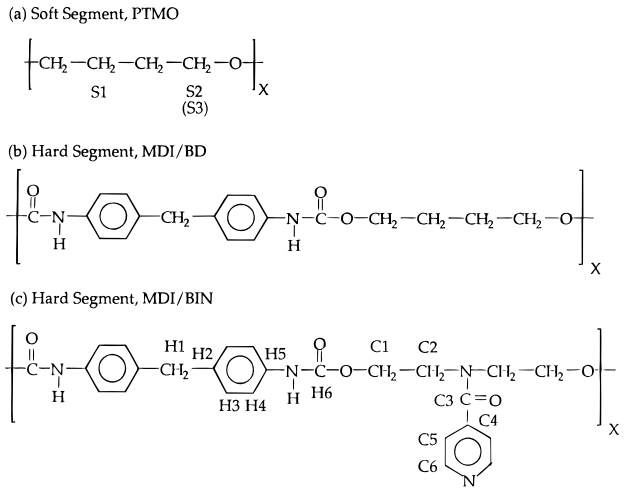


**Figure 1.** Schematics of the polyurethane soft segment (PTMO) and two hard segments, (b) MDI/BD and (c) MDI/BIN. The letters below the schematics such as "S1" refer to Table 1 and Figure 3.

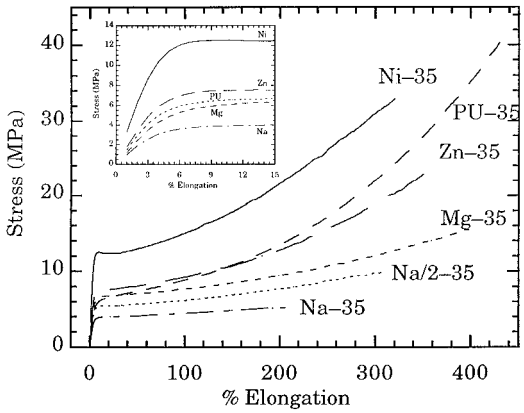


**Figure 2.** Stress−strain curves for PU-35 and its blends with nickel, zinc, magnesium, and sodium acetates. Sample Na/2−35 has half the stoichiometric amount of sodium. The inset shows the initial slopes.

than those presented in an earlier study;[12] this discrepancy is most likely due to aging of the polyurethanes and possibly the effects of annealing since these samples were dried at 50−60 °C both in air and under vacuum to completely remove the solvent, DMF. The strain hardening seen in PU-35 and Zn-35 is likely due to crystallization of the PTMO soft segment. It is apparent that blending dramatically improves both the modulus and ultimate strength of the polyurethane. It is proposed that the improvements in mechanical strength are due to the metal acetate complexing with the pyridine nitrogen on a molecular level. This supposition can be tested using spectroscopic methods.

**Polyurethanes and Blends with Transition Metals. $^{13}$C NMR Chemical Shifts and Cross-Polarization.** The solid-state $^{13}$C NMR spectrum of PU-35 is shown in Figure 3; the corresponding peak identification is in Table 1. Peak identification is based on known polyurethane spectra,[19,20] small molecules,[21,22] and the $^{13}$C solution-state spectrum.[12]

The $^{13}$C CPMAS NMR spectra of PU-35 and Zn-35 are shown in Figure 4. From Figure 2 it is apparent that blending with transition-metal salts such as nickel acetate have the largest effect on the mechanical properties of the polyurethane. However, nickel is paramagnetic and relaxes all nuclei in its immediate area, and all NMR signals from nearby carbons and

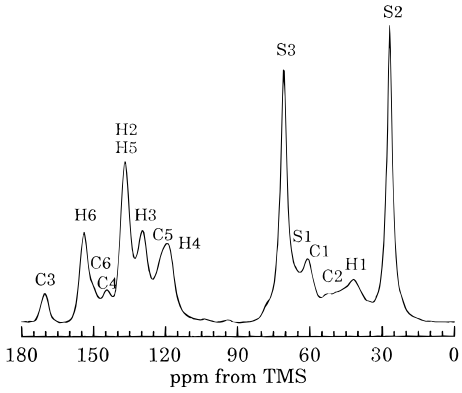


**Figure 3.** $^{13}$C NMR spectrum of PU-35. Peak identification corresponds to Table 1 and Figure 1.

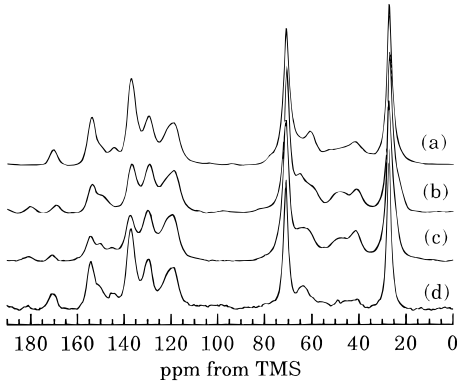


**Figure 4.** $^{13}$C NMR spectra of (a) PU-35, (b) Zn-35 (c) Mg-35, and (d) Na/2−35. The contact times were either 0.5 or 1 ms. Spectrum d was collected with slightly different NMR conditions (2 ms spin-lock time).

**Table 1. $^{13}$C NMR Peak Assignments for PU-35**

| carbon site | carbon label | shift (ppm) |
|---|---|---|
| PTMO external $CH_2$ adjacent to urethane | S1 | 65 |
| PTMO internal $CH_2$ | S2 | 27 |
| PTMO external $CH_2$ | S3 | 71 |
| MDI $CH_2$ | H1 | 41 |
| MDI quaternary ring | H2/H5 | 137 |
| MDI internal protonated ring | H3 | 129 |
| MDI external protonated ring | H4 | 119 |
| MDI urethane carbonyl | H6 | 154 |
| chain-extender external $CH_2$−O | C1 | 61 |
| chain-extender internal $CH_2$−N | C2 | 49 |
| chain-extender carbonyl | C3 | 170 |
| pyridine quaternary aromatic | C4 | 144 |
| pyridine protonated aromatic | C5 | 123 |
| pyridine protonated aromatic adjacent to nitrogen | C6 | 150 |

nitrogens are lost. Zinc is not paramagnetic, and quantitative information on blends with zinc acetate can be obtained. The difference in the mechanical properties of blends with these two transition metals is likely due to the differences in complexation between nickel ($d^8$ complex) and zinc ($d^{10}$ complex).[11,23]

In Figure 4 there is an additional peak at 181 ppm in Zn-35 that is not present in PU-35 which is due to the carbonyl carbon of the zinc acetate group; the methyl group is incorporated into the 27 ppm peak. The peak position of the acetate carbonyl carbon is 3 ppm upfield from the unblended zinc acetate (184 ppm). Blends with the chain extender and hard segment also show this carbonyl shift (Table 2). A similar shift in the zinc acetate carbonyl region has been seen previously[11] in blends of P4VP and zinc acetate. This peak shift was

**Table 2. Chemical Shifts (Widths) for the Metal Acetates (ppm)**

| | neat | blend with BIN | blend with MDI/BIN | blend with PU-35 |
|---|---|---|---|---|
| zinc acetate | 184 (0.5) | 179 (1.3)<br>183.5 (0.8) | 179.5 (1.9) | 181 (1.9) |
| magnesium acetate | 183 (0.5) | 180.5 (3.2) | 179.5 (2.5) | 181 (2.0) |
| sodium acetate | 182 (0.5) | | 183 (1.5) | 183 (2.5)<br>182 (1.4)[a] |

[a] Sample Na/2, with half the stoichiometric amount of sodium acetate.

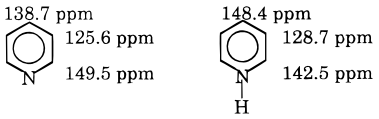


**Figure 5.** Peak identification of carbon sites in pyridine and pyridinium ion.

attributed to transition-metal complexation. Additionally, there are other qualitative changes in the polyurethane spectrum after blending. The peak at 144 ppm (due to the pyridine quaternary aromatic carbon) has shifted, probably downfield. According to Levy *et al.*,[22] protonation of a pyridine nitrogen will increase the chemical shift of the carbon in the para position (Figure 5). Complexation with zinc should cause a shift in the same direction. The peak at 150 ppm (due to the carbon adjacent to the pyridine nitrogen) has sharpened and shifted slightly upfield, which is also consistent with data from Levy *et al.*[22] The other pyridine ring carbons overlap with the MDI carbons of the polyurethane. The position of the chain-extender carbonyl peak has shifted upfield ~1 ppm, to 169 ppm. Finally, the NMR peak due to the urethane carbonyl (H6, at 154 ppm) does not shift with blending, indicating no interaction is occurring at the urethane carbonyl site. Similar results are seen in the hard-segment materials.

The cross-polarization dynamics have changed in the aromatic region upon the addition of zinc acetate, leading to a change in the ratios of the peaks. Changes such as these can also be caused by drying the samples thoroughly so that most water is removed. With this type of drying procedure, the intensity of the peak at 144 ppm is suppressed, but not removed, because the residual water provides nearby protons for cross-polarization of the quaternary carbon.

When the materials are exposed to equivalent humidity levels so the effects of water content are minimized, blending causes changes in the cross-polarization dynamics of the aromatic region, as seen in Figure 4. The peaks in the range 30−70 ppm have changed as well; the peak due to the chain-extender $CH_2$−N has become more prominent and the peaks due to the chain-extender $CH_2$−O carbons and the PTMO end groups (61 and 65 ppm, respectively) have either shifted or broadened. These changes can only be discussed qualitatively, however, because the spinning sidebands of the aromatic regions overlap with these sites. Obviously, blending has affected the dynamics and local electron structure of the polyurethane. The effect of blending on the chemical shifts and cross-polarization dynamics can be taken as indirect evidence of complexation.

**$^{13}$C Relaxation Times.** Spin−lattice relaxation times in the rotating frame ($T_{1\rho}$) were acquired to determine the effects of blending on the kilohertz frequency motions of the polyurethane carbon nuclei. $T_{1\rho}$ values have been shown to give the most information on motions in polyurethane and poly(urethane−urea) systems.[19,24] Polyurethanes are phase-separated systems and because of that generally have two relaxation times for each type of carbon nucleus. The $T_{1\rho}$ relaxation plots were fit using a two-component model:

$$M(t) = M_f \exp\left(-\frac{t}{T_{1\rho f}}\right) + M_s \exp\left(-\frac{t}{T_{1\rho s}}\right) \qquad (1)$$

where $M_f$ and $M_s$ are the magnetizations of the two different components (fast and slow) and $T_{1\rho,f}$ and $T_{1\rho,s}$ are the corresponding relaxation times. For example, the urethane carbonyl may have two components to the relaxation curve. In that case, one component is likely due to the carbonyl carbons in the hard domain, while the other is due to carbonyls at the interface of the hard and soft domains or dissolved in the soft phase. Previous work in this laboratory[19] concluded that the longer $T_{1\rho}$ component in poly(ether−urethanes) could be assigned to carbons in the hard domain. Since this work focuses on changes in the hard domain of the polyurethane, the emphasis will be on these longer $T_{1\rho}$ times.

Blending with zinc acetate has an effect on the relaxation dynamics of the polyurethane. Tables 3 and 4 contain both components of the $T_{1\rho}$ relaxation curves for PU-35 and Zn-35 and the fractions of the slowly relaxing components from the relaxation curves ($M_s/M_t$, where $M_t$ is the total magnetization). Following blending with zinc acetate, the relaxation times of all carbon sites in the hard segment increase. Addition of the zinc acetate decreases the segmental motion near the 45 kHz spin-locking frequency; the correlation times of the carbon nuclei increase and the $T_{1\rho}$ values increase. These increases indicate that blending restricts the motion of the carbons within the hard domain.

The relative fractions of carbon sites in the slow-component regime have either remained constant or increased slightly after the addition of zinc acetate, indicating that the amount of phase separation may increase slightly but has not changed dramatically with blending. This is consistent with previous studies on these materials.[12,13] The fraction $M_s/M_t$ for the pyridine carbon adjacent to the nitrogen (150 ppm) has increased substantially, about 85%. This carbon is closest to the nitrogen, which is the proposed site of the complexation; therefore, it is fitting that this carbon is the most affected, since more pyridine groups are motionally

**Table 3. Spin−Lattice Relaxation Times in the Rotating Frame ($T_{1\rho}$) for PU-35**

| carbon site | shift (ppm) | $M_f$ | $T_{1\rho,f}$ (ms) | $M_s$ | $T_{1\rho,s}$ (ms) | $M_s/M_t$ |
|---|---|---|---|---|---|---|
| MDI external protonated ring | 119 | 42100 | 1.16 | 18800 | 15.7 | 0.309 |
| MDI internal protonated ring | 129 | 73600 | 1.33 | 24400 | 12.1 | 0.248 |
| MDI quaternary ring | 137 | 35500 | 0.56 | 83900 | 20.6 | 0.703 |
| MDI urethane carbonyl | 154 | 8430 | 0.36 | 38700 | 23.4 | 0.821 |
| pyridine protonated aromatic | 122 | 41600 | 1.02 | 12200 | 16.7 | 0.227 |
| pyridine quaternary aromatic | 145 | 1160 | 0.57 | 3440 | 31.0 | 0.748 |
| pyridine protonated aromatic adjacent to nitrogen | 150 | 17200 | 0.94 | 8680 | 19.8 | 0.335 |
| chain-extender carbonyl | 170 | 1920 | 0.32 | 1000 | 24.9 | 0.839 |
| acetate salt carbonyl | 181 | | | | | |

**Table 4. Spin−Lattice Relaxation Times in the Rotating Frame ($T_{1\rho}$) for Zn-35**

| carbon site | shift (ppm) | $M_f$ | $T_{1\rho,f}$ (ms) | $M_s$ | $T_{1\rho,s}$ (ms) | $M_s/M_t$ |
|---|---|---|---|---|---|---|
| MDI external protonated ring | 119 | 14600 | 2.00 | 7030 | 20.8 | 0.325 |
| MDI internal protonated ring | 129 | 17800 | 2.09 | 9780 | 15.8 | 0.355 |
| MDI quaternary ring | 137 | 5480 | 2.53 | 17300 | 33.9 | 0.759 |
| MDI urethane carbonyl | 154 | 1270 | 2.56 | 8400 | 37.8 | 0.869 |
| pyridine protonated aromatic | 122 | 6410 | 1.58 | 3600 | 23.4 | 0.360 |
| pyridine quaternary aromatic | 145 | | | | | |
| pyridine protonated aromatic adjacent to nitrogen | 150 | 3440 | 2.45 | 5630 | 27.2 | 0.621 |
| chain-extender carbonyl | 170 | 614 | 2.21 | 2600 | 44.3 | 0.809 |
| acetate salt carbonyl | 181 | | | | | |

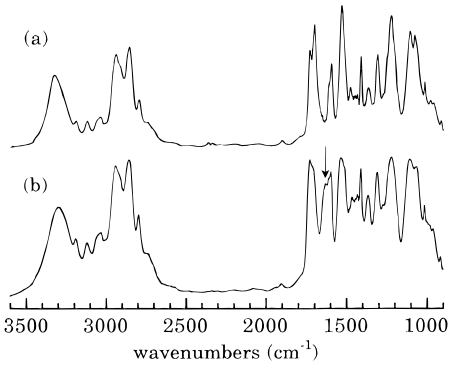


**Figure 6.** FTIR spectra of (a) Pellethane, a commercial poly(ether−urethane), and (b) PU-35. The arrow points to the 1630 $cm^{-1}$ band.

restricted after blending than before. The other protonated aromatic carbon in the pyridine ring also shows an increase in the fraction of the slow component. Finally, the carbonyl carbon of the chain extender, while not affected dramatically in $M_s/M_t$, does show substantial increases in both $T_{1\rho}$ values. If the pyridine ring flips are suppressed by the complexation, this may decrease the fluctuating magnetic fields near the carbonyl carbon and cause an increase in the relaxation time.

**Infrared Spectroscopy.** Fourier transform infrared spectroscopy (FTIR) is used extensively in the study of specific interactions in polymer blends.[25,26] In Figure 6, the infrared spectrum of PU-35 is compared with the spectrum of a commercial poly(ether−urethane) (Pellethane, Dow Chemical, having a component ratio of roughly 3/2/1 MDI/BD/PTMO), which does not contain the pyridine group. A band appears near 1630 $cm^{-1}$ in PU-35. This peak appears only in materials containing the pyridine-containing chain extender and is assigned to the pyridine group. Other researchers have identified a band due to the pyridine C−N stretch near 1600 $cm^{-1}$;[27−29] however, this region contains many overlapping bands and a positive identification cannot be achieved. FTIR bands due to pyridinium ions are found near 1636 $cm^{-1}$;[27−29] the possibility of a similar structure in these polyurethanes is investigated by $^{15}N$ NMR and discussed below.

Incorporation of the pyridine group into the polyurethanes also affects the hydrogen bonding in the materials. The ratios of free and hydrogen-bonded carbonyls (1730 and 1703 $cm^{-1}$, respectively)[30] change when the pyridine-containing chain extender is incorporated into the material, although some of the change in the carbonyl ratio is due to the presence of the chain-extender carbonyl. The N−H stretching region contains a collection of bands in polyurethanes.[30−34] The maximum of the broad N−H band shifts with the incorporation of pyridine, indicating a change in the relative ratios of types of N−H stretches. A more complete discussion of hydrogen bonding in these pyridine-containing polyurethanes can be found elsewhere.[35] Pyridine and urethane N−H band positions for the base materials and several of the polyurethane blends are shown in Table 5.

**Table 5. FTIR Band Positions for Pyridine-Containing Polyurethanes and Blends**

| sample i.d. | wavenumber, pyridine group ($cm^{-1}$) | wavenumber, H-bonded N−H ($cm^{-1}$) |
|---|---|---|
| MDI/BD | | 3328 |
| MDI/BIN | 1630 | 3287 |
| MDI/BIN/Zn | 1634 | 3301 |
| MDI/BIN/Mg | 1633 | 3300 |
| MDI/BIN/Na | 1629 | 3293 |
| Pellethane | | 3329 |
| PU-29 | 1630 | 3296 |
| Zn-29 | 1644 | 3304 |
| Ni-29 | 1635 | 3303 |
| PU-35 | 1630 | 3295 |
| Zn-35 | 1632 | 3302 |
| Mg-35 | 1626 | 3300 |
| Na-35 | 1626 | 3300 |
| Ni-35 | 1632 | 3300 |

From the data in Table 5 it is apparent that blending with transition metals such as zinc and nickel leads to a slight increase in wavenumbers of the band corresponding to the pyridine group (1630 $cm^{-1}$). Blending with the metals should disrupt the >N:···H−N hydrogen bonding, so the N−H stretch should shift as well. This shift to higher wavenumbers does occur with blending. Skrovanek *et al.*[36] have described the frequency of the peak maximum in the N−H stretching region of a polyamide as due to an average of all N−H hydrogen bond strengths. This idea can be extended to materials with many hydrogen-bonding sites, such as these pyridine-containing polyurethanes. Complexation between the pyridine nitrogen and metal ion effectively removes a possible hydrogen bonding site for the urethane N−H group, a site which is at lower frequency than the C═O···H−N bond, so the average position of the N−H stretching band moves to a higher frequency. This is consistent with the findings from $^{15}N$ NMR which will be discussed below.

**$^{15}N$ NMR Chemical Shifts and Cross-Polarization.** FTIR and $^{13}C$ NMR studies give indirect evidence for complexation in these blends. A much more direct probe is $^{15}N$ NMR of the possible complexing nucleus, the pyridine nitrogen. Figure 7 shows the natural-abundance (0.37% of all N) $^{15}N$ CPMAS NMR spectrum of the MDI/BIN hard-segment material. The polyurethanes themselves were not examined because of the prohibitively low amount of $^{15}N$ they contain. At different cross-polarization times, different peaks are emphasized. $^{15}N$ peaks are seen at −276, −320, and possibly −405 ppm.

The peaks were identified by comparing the positions to other urethane and pyridine-containing materials. Figure 8 shows the NMR spectra of MDI/BD, which contains only urethane nitrogens at −281 ppm, and the

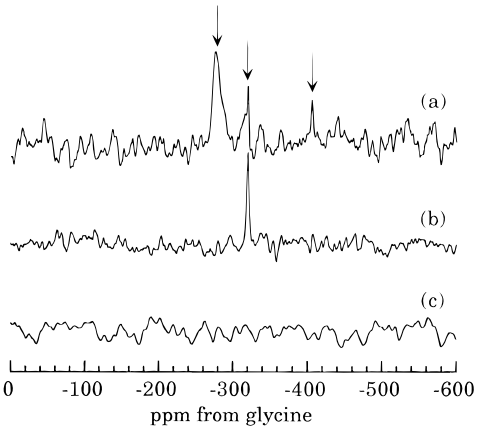


**Figure 7.** $^{15}$N NMR spectra of MDI/BIN at three contact times: (a) 0.5, (b) 2, and (c) 3 ms.

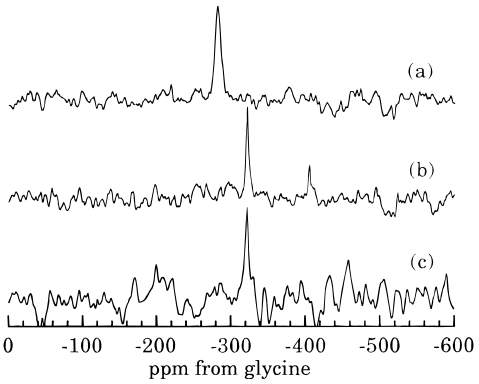


**Figure 8.** $^{15}$N NMR spectra of (a) MDI/BD, (b) BIN, and (c) P4VP.

NMR spectrum of BIN, the chain extender. The two spectra contain all the peaks present in the MDI/BIN material. Therefore, the −276 ppm peak is assigned to the urethane nitrogens; this assignment agrees with many in the literature.[37] The slight shift of the urethane nitrogen, from −281 to −276 ppm, may be an artifact of the signal-to-noise level, or it may be due to the different types of hydrogen bonding in the two materials.

The spectrum of P4VP is shown in Figure 8c. It shows a single peak at −322 ppm, which is comparable to one of the peaks seen in BIN, and this peak is assigned to the pyridine nitrogen. The assignment of the third peak in MDI/BIN, at −405 ppm, is discussed below. It could be due to the amide nitrogen in the chain extender (BIN), but is far upfield from most amide shifts.[37,38] It is also possible that the −405 ppm peak is due to a pyridinium-type nitrogen that is hydrogen bonded to OH groups (in BIN) or urethane N−H groups (in MDI/BIN). The pyridinium ion resonates about 100 ppm upfield from pyridine nitrogen,[38] and a hydrogen-bonded pyridine group may show a slightly smaller shift compared to the pyridinium ion. Therefore, the ∼80 ppm shift from pyridine is reasonable for this species. FTIR experiments indicated the presence of hydrogen bonding to the pyridine nitrogen, so it is most likely that this peak is due to hydrogen-bonded pyridine nitrogen. If this −405 ppm peak is due to hydrogen-bonded pyridine nitrogen, then there are no remaining unassigned peaks in the NMR spectrum of MDI/BIN and it appears that the amide nitrogens in the polymer backbone are not detected with these cross-polarization parameters. However, it is the pyridine nitrogen peak which is of greatest interest in this study.

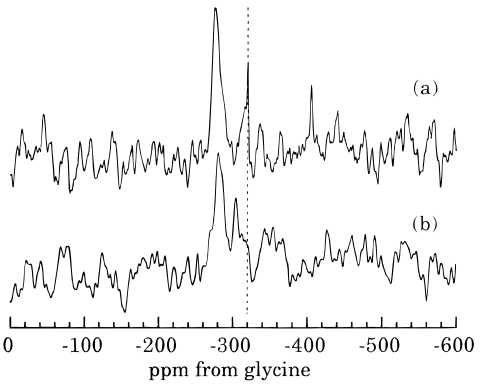


**Figure 9.** $^{15}$N NMR spectra of (a) MDI/BIN at a contact time of 0.5 ms and (b) MDI/BIN/Zn at a contact time of 5.5 ms.

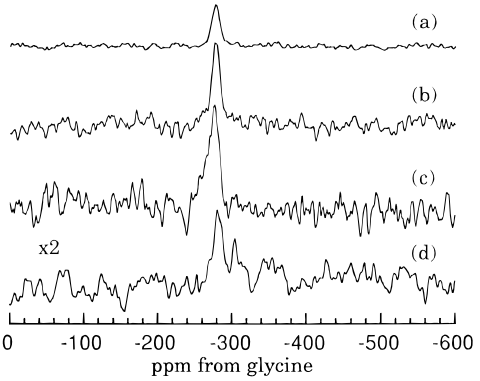


**Figure 10.** $^{15}$N NMR spectra of MDI/BIN/Zn at four contact times: (a) 0.7, (b) 1.7, (c) 3, and (d) 5.5 ms. Spectral intensities are normalized.

MDI/BIN was blended with zinc acetate and the $^{15}$N NMR spectra were acquired. $^{13}$C NMR spectra were taken to ensure that little if any residual solvent (DMF) was present. Figure 9 shows the $^{15}$N NMR spectrum of the blend compared with that of the original hard-segment material. Other researchers[39] have proposed that interactions can take place at either the urethane carbonyl carbon or the pyridine nitrogen. Since no significant shift is apparent in the urethane carbonyl group (Figure 4) or the urethane nitrogen immediately neighboring it, the interaction is not at that site. Instead, the peak due to the pyridine nitrogen has shifted significantly downfield, from −320 to −304 ppm. Additionally, the −405 ppm peak has disappeared. This peak has been identified as due to hydrogen-bonded pyridine nitrogens, and during blending the proton involved in hydrogen bonding has been displaced by the zinc in the acetate. This result is consistent with the presence of a peak shift of the urethane N−H FTIR band in after blending (Table 5), since the N−H group would be the band involved in hydrogen bonding. The changes in the NMR spectrum with blending are direct evidence that complexation has taken place at the pyridine site.

Blending also affects the cross-polarization dynamics of the polyurethane. Figure 7 shows the $^{15}$N NMR spectra of MDI/BIN at several different contact times. The urethane nitrogen cross polarizes at shorter contact times than the pyridine nitrogen, and both signals are short-lived, vanishing by a contact time of 3 ms. In contrast, Figure 10 shows the spectra of MDI/BIN/Zn at several contact times. The dynamics are quite different from what was seen for MDI/BIN. Once again the urethane nitrogen cross-polarized at shorter contact times than the pyridine group; however, the peak

persists to much higher contact times in the blend. Additionally, the contact time at which the pyridine nitrogen appears has increased dramatically; now the peak appears at much longer times (5.5 ms). The increase in the contact time for the pyridine nitrogen is due to the complexation; nearby protons have been displaced by the zinc atom, and cross-polarization is more difficult. The change in the contact time dynamics of the urethane nitrogen is probably due to the change in hydrogen bonding that affected the N−H stretch in the FTIR spectra.

**Blends with Non-Transition Metals.** The previous studies on pyridine-containing blends have focused mainly on transition-metal complexes. One of the purposes of this study is to determine the local interactions of a transition metal (zinc) with the pyridine nitrogen. Additionally, the effects of a non-transition metal (magnesium) on the properties of this polyurethane are also of interest. In previous studies of poly(4-vinylpyridine),[6,7,11] magnesium did not complex with the pyridine nitrogen. Belfiore *et al.*[11] reported $^{13}C$ NMR chemical shifts of the acetate carbonyl peak in blends of zinc acetate and P4VP as an indication of complexation, and no such shifts were present in blends of magnesium acetate and P4VP. In the PU-35 system, however, a distinct shift in the acetate peak is apparent when neat magnesium acetate is compared to its blend with PU-35 (Table 2). However, the qualitative changes in the $^{13}C$ spectrum of Mg-35 after blending are not as distinctive as in the blend with zinc acetate. In particular, the pyridine C−N carbon at 144 ppm and chain-extender carbonyl at 170 ppm are not affected as dramatically (Figure 4). Additionally, X-ray experiments showed no changes in the SAXS pattern of PU-35 when blended with magnesium acetate.

Tensile tests indicate that magnesium does affect the tensile properties of the polyurethane, albeit slightly (Figure 2). The increase in modulus for the magnesium blend is not considered to be a filler effect because the $^{13}C$ NMR data indicate that the acetate peak shifts from 183 to 181 ppm, similar to the shift in Zn-35 (Table 2 and Figure 4). Additionally, blending with sodium acetate decreases the modulus of the material. The NMR position of the sodium acetate carbonyl does not change after blending with sodium acetate; if anything, it actually shifts in the opposite direction from that seen in all other blends (Table 2).

It is possible that the magnesium ion interacts with a group other than the pyridine nitrogen, such as the amine nitrogen or the carbonyl group. Interaction with the urethane carbonyl is unlikely since its chemical shift at 154 ppm is unchanged from PU-35 (Figure 4). The $^{15}N$ NMR of MDI/BIN/Mg is shown in Figure 11. The pyridine nitrogen shifts 11 ppm relative to MDI/BIN, to ∼−309 ppm. This shift is similar to that seen in the zinc blend, in which the pyridine peak shifted to −304 ppm. It appears that magnesium does affect the pyridine nitrogen, but the interaction is not as strong as in the blend with zinc acetate. Additionally, the cross-polarization dynamics of the urethane nitrogen in the blend with magnesium acetate (Figure 11) are different from that in the blend with zinc acetate (Figure 10). In MDI/BIN/Mg, the maximum intensity is found near a contact time of 0.7 ms. This maximum in the cross-polarization curve of the urethane nitrogen is much closer to the maximum seen in MDI/BIN (near 0.5 mg, Figure 7) than in MDI/BIN/Zn (near 3 ms, Figure 10). In both blends the signal persists to much higher contact

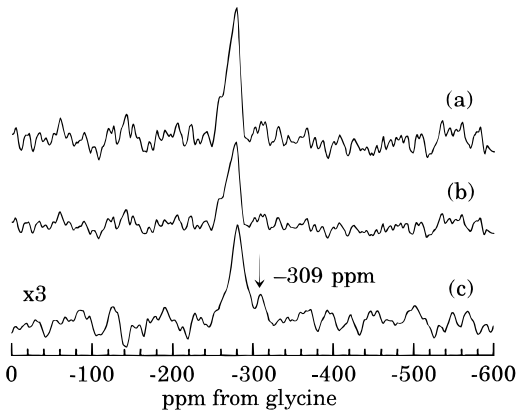


**Figure 11.** $^{15}N$ NMR spectra of MDI/BIN/Mg at three different contact times: (a) 0.7, (b) 2, and (c) 5.5 ms. Spectral intensities are normalized.

times than in the original unblended hard-segment material. Lu and Weiss[8] found miscible, interacting blends of certain ratios of Zn- and Na-neutralized SPS and PSVP blended in DMF, cast, and annealed. One glass-transition temperature ($T_g$) was seen for some ratios, and for other ratios the individual $T_g$'s were functions of composition, indicating some interaction. From their study and the present $^{13}C$ and $^{15}N$ NMR chemical shifts, interactions between pyridine and non-transition metal ions such as magnesium are shown to be possible, but the mechanism is different and the interaction is weaker than that in transition-metal blends.

The FTIR data in Table 5 show the shifts of the pyridine band and urethane N−H group when acetate salts are incorporated into the polyurethane PU-35 and the hard-segment material. The pyridine bands in blends with sodium acetate appear at lower wavenumbers than in MDI/BIN, PU-35, and most other blends. Only Mg-35 has an equivalent band position to Na-35 (Table 5). For the hard segments in all other blends, including that with magnesium, the pyridine bands have higher positions. The position of the maximum in the N−H stretching band is also lower in MDI/BIN/Na than in all other hard-segment blends. This probably indicates that the metal−pyridine interaction that increased the band position in the other blends is not present in the sodium blend. Finally, the sodium-containing materials have an additional peak at 1572 $cm^{-1}$, which is not present in any other starting polymer or blend. Carboxylate anion peaks are generally found around 1550 $cm^{-1}$.[40] In sodium-neutralized ethylene−methacrylate polymers, Brozoski *et al.*[40] identified two IR bands in this region, at 1547 and 1568 $cm^{-1}$. They reported the position of this peak to be a function of cation type and local structure. The appearance of this peak in only the sodium blends could indicate that the local structure in these blends is different than in the other metal-containing materials.

In Figure 2, the polyurethane blended with sodium acetate shows decreased mechanical properties compared to the unblended polymer. Sodium is a monovalent ion that probably needs to cluster in order to form physical crosslinks. Unlike ionomers, the sodium incorporated into these materials is present as a separate molecule (sodium acetate) and not ionically bonded to the polymer chain. Aggregation of the sodium groups could lead to clusters of sodium acetate that would not cross-link the polymer chains, but instead would lower the mechanical properties of the polyurethane.

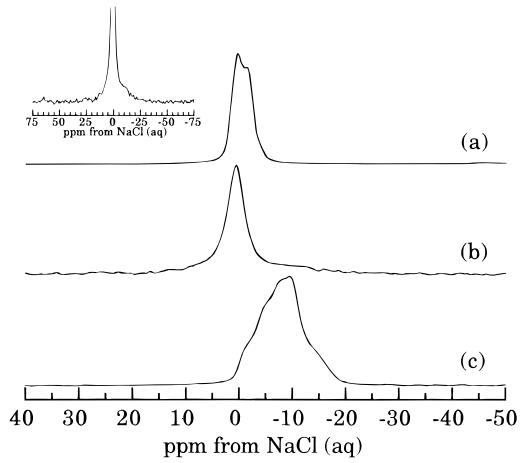


**Figure 12.** $^{23}$Na NMR of (a) sodium acetate, (b) Na-35, and (c) MDI/BIN/Na. The inset is an expanded view of (b).

$^{23}$Na NMR experiments were completed on the sodium-containing polyurethane materials to determine the environment of the sodium in these materials. Figure 12 shows the results of these experiments. Sodium acetate (Figure 12a) is characterized by a broadened quadrupolar line shape centered near 0 ppm. After blending with PU-35, the main peak is shifted slightly downfield and is Lorentzian in shape, but there is also a very small amount of intensity at lower ppm (Figure 12 inset), characterized by a broad peak. The narrow peak is most likely due to amorphous sodium acetate; the loss of crystalline structure would lead to a more average environment around the sodium and a decrease in the quadrupole coupling constant. The broad peak is probably equivalent to the aggregated sodium ions in sodium-neutralized sulfonated polystyrene ionomers.[41] Evidently there are relatively few clustered sodium ions (~20%) in this polyurethane blend, so the sodium acetate is not contributing significantly to mechanical properties. Instead, it is most likely acting as a diluent or plasticizer within the hard domain. It is possible, however, that the few clusters that do exist would contribute to early failure of the material. The behavior in the hard-segment material is quite different (Figure 12c). The sodium acetate has a new local structure so the peak shifts upfield from the neat sodium acetate, similar to the behavior in ionomers.[41] This shift could be due to some clustering or phase separation of the sodium acetate. This hard-segment blend was more opaque than all other blends, possibly due to poor compatibility of the sodium acetate and the polyurethane. Agarwal *et al.*[7] reported a gradual decrease in clarity for blends of PSVP and metal-neutralized S-EPDM when the metal was varied from zinc to magnesium and then to sodium, the last of which was completely opaque. The PSVP blends containing magnesium and sodium did not show any indications of complexation.

$^{13}$C NMR studies of both MDI/BIN/Na and Na-35 were undertaken. Incorporation of sodium does not affect the $^{13}$C spectrum of the polyurethane materials in the same way that occurs upon blending with zinc or magnesium acetate. The peak at 144 ppm is still present for the sodium blends and the 150 ppm carbon is also unaffected (Figure 4). Additionally, the acetate carbonyl in Na-35 does not change position compared to the neat sodium acetate peak (Table 2). The carbonyl in sodium acetate also has a much lower cross-polarized intensity than the carbonyls in all other blends, indicating that its environment is not equivalent to the others. The acetate carbonyl in MDI/BIN/Na may have shifted slightly downfield compared to the unblended salt, but the peak width is larger than the possible shift, so the extent of the shift is near the limit of resolution. Finally, $^{15}$N NMR results showed a very weak CPMAS peak at ~−323 ppm with a contact time of 9 ms. Therefore, the position of the pyridine nitrogen in MDI/BIN does not change when the polyurethane is blended with sodium, and no complex is formed.

$^{23}$Na, $^{13}$C, and $^{15}$N NMR data indicate that the sodium acetate in these blends is not forming any complex with the pyridine nitrogen of the chain extender. In order to form physical cross-links, most likely the sodium ions must form aggregates similar to those seen in ionomers; however, because the sodium is monovalent and part of an acetate group, it cannot coordinate with the acetate groups and the pyridine nitrogen simultaneously. Instead, it remains mostly isolated in the case of Na-35, in which the number of sodium acetates per gram of polymer is much lower than in the hard-segment material. In the hard-segment material, the sodium acetate is able to aggregate together, probably into separate domains.

## Conclusions

$^{15}$N NMR gives direct evidence for metal−pyridine interactions in blends of pyridine-containing polyurethanes and metal acetates. After blending with zinc acetate, the pyridine nitrogen peak shifts from −320 to −304 ppm. In $^{13}$C NMR studies, the acetate carbonyl and pyridine ring carbons shift after blending, offering indirect evidence of complexation. Relaxation studies show increases in $T_{1\rho}$ values when zinc acetate is blended with the polyurethane. This is due to complexation with the metal cation which decreases segmental motions of the hard-domain carbons in the kilohertz frequency range. The effects of incorporation of the pyridine group on the hydrogen bonding within the hard domain are apparent in FTIR experiments. Effects of blending with zinc acetate on the hard-domain hydrogen bonding were evident in FTIR and $^{15}$N NMR contact-time experiments. The IR N−H stretching band shifts to higher wavenumbers and the $^{15}$N NMR N−H signal persists to higher contact times for the blend. Blends of polyurethanes and magnesium acetate also cause shifts in the $^{13}$C and $^{15}$N NMR spectra, but not to the extent seen in blends with zinc acetate. Sodium acetate does not complex with the BIN-containing polyurethanes; no shifts in the $^{13}$C NMR signal for the acetate carbonyl or in the $^{15}$N NMR for the pyridine nitrogen are apparent.

**Acknowledgment.** The authors would like to thank Richard J. Goddard for synthesizing the MDI/BD hard-segment material. The solid-state NMR spectrometer used in this work was purchased with financial support from Shell Oil Foundation. Additional funding for this research was obtained through Grant DMR-9016959 from the National Science Foundation. E.M.O. also would like to acknowledge fellowship support from the Department of Defense (National Defense and Engineering Graduate Fellowship program) and the support of the American Association of University Women.

## References and Notes

(1) Agnew, N. H. *J. Polym. Sci., Polym. Chem. Ed.* **1976**, *14*, 2819.

(2) Meyer, C. T.; Pineri, M. *J. Polym. Sci., Polym. Phys. Ed.* **1975**, *13*, 1057.
(3) Pineri, M.; Meyer, C.; Bourret, A. *J. Polym. Sci., Polym. Phys. Ed.* **1975**, *13*, 1881.
(4) Meyer, C. T.; Pineri, M. *J. Polym. Sci., Polym. Phys. Ed.* **1978**, *16*, 569.
(5) Meyer, C. T.; Pineri, M. *Polymer* **1976**, *17*, 382.
(6) Peiffer, D. G.; Duvdevani, I.; Agarwal, P. K.; Lundberg, R. D. *J. Polym. Sci., Polym. Lett. Ed.* **1986**, *24*, 581.
(7) Agarwal, P. K.; Duvdevani, I.; Peiffer, D. G.; Lundberg, R. D. *J. Polym. Sci., Polym. Phys. Ed.* **1987**, *25*, 839.
(8) Lu, X.; Weiss, R. A. *Macromolecules* **1991**, *24*, 5763.
(9) Belfiore, L. A. *Polym. Prepr.* (*Am. Chem. Soc., Div. Polym. Chem.*) **1988**, *29*, 17.
(10) Belfiore, L. A.; Graham, H.; Ueda, E. *Macromolecules* **1992**, *25*, 2935.
(11) Belfiore, L. A.; Pires, A. T. N.; Wang, Y.; Graham, H.; Ueda, E. *Macromolecules* **1992**, *25*, 1411.
(12) Yang, C.-Z.; Zhang, X.; O'Connell, E. M.; Goddard, R. J.; Cooper, S. L. *J. Appl. Polym. Sci.* **1994**, *51*, 365.
(13) Grady, B. P.; O'Connell, E. M.; Yang, C.-Z.; Cooper, S. L. *J. Polym. Sci., Polym. Phys. Ed.* **1994**, *32*, 2357.
(14) Powell, D. G.; Sikes, A. M.; Mathias, L. J. *Polymer* **1991**, *32*, 2523.
(15) Chuang, I.-S.; Maciel, G. E. *Polymer* **1994**, *35*, 1621.
(16) Koenig, J. L. *Spectroscopy of Polymers*; American Chemical Society: Washington, DC, 1992.
(17) Lippmaa, E.; Samoson, A.; Magi, M. *J. Am. Chem. Soc.* **1986**, *108*, 1730.
(18) Samoson, A.; Lippmaa, E. *Phys. Rev. B* **1983**, *28*, 6567.
(19) Okamoto, D. T.; O'Connell, E. M.; Cooper, S. L.; Root, T. W. *J. Polym. Sci., Polym. Phys. Ed.* **1993**, *31*, 1163.
(20) Meadows, M. D.; Christenson, C. P.; Howard, W. L.; Harthcock, M. A.; Guerra, R. E.; Turner, R. B. *Macromolecules* **1990**, *23*, 2440.
(21) *Handbook of $^{13}C$ NMR Spectra*; Toda, F., Ed.; Sanyo: Tokyo, 1981.
(22) Levy, G. C.; Lichter, R. L.; Nelson, G. L. *Carbon-13 Nuclear Magnetic Resonance Spectroscopy*, 2nd ed.; John Wiley & Sons: New York, 1980.
(23) Belfiore, L. A.; Graham, H.; Ueda, E. *Macromolecules* **1992**, *25*, 2935.
(24) Okamoto, D. T.; Cooper, S. L.; Root, T. W. *Macromolecules* **1992**, *25*, 1068.
(25) Coleman, M. M.; Graf, J. F.; Painter, P. C. *Specific Interactions and the Miscibility of Polymer Blends*; Technomic Publishing Co.: Lancaster, PA, 1991.
(26) Coleman, M. M.; Painter, P. C. *Appl. Spectrosc. Rev.* **1984**, *20*, 255.
(27) Smith, P.; Eisenberg, A. *Macromolecules* **1994**, *27*, 545.
(28) Sakurai, K.; Douglas, E.; MacKnight, W. J. *Macromolecules* **1992**, *25*, 4506.
(29) Sakurai, K.; Douglas, E.; MacKnight, W. J. *Macromolecules* **1993**, *26*, 208.
(30) Seymour, R. W.; Estes, G. M.; Cooper, S. L. *Macromolecules* **1970**, *3*, 579.
(31) Srichatrapimuk, V. W.; Cooper, S. L. *J. Macromol. Sci., Phys.* **1978**, *B15*, 267.
(32) Lee, H. S.; Wang, Y. K.; Hsu, S. L. *Macromolecules* **1987**, *20*, 2089.
(33) Goddard, R. J.; Cooper, S. L. *Macromolecules* **1995**, *28*, 1390.
(34) Bandekar, J.; Klima, S. *J. Mol. Struct.* **1991**, *263*, 45.
(35) O'Connell, E. M. Ph.D. Dissertation, University of Wisconsin—Madison, 1995.
(36) Skrovanek, D. J.; Painter, P. C.; Coleman, M. M. *Macromolecules* **1986**, *19*, 699.
(37) Duncan, T. M. *A Compilation of Chemical Shift Anisotropies*; The Farragut Press: Chicago, 1990.
(38) Levy, G. C.; Litcher, R. L. *Nitrogen-15 Nuclear Magnetic Spectroscopy*; John Wiley & Sons: New York, 1979.
(39) Kwei, T. K.; Dai, Y. K.; Lu, X.; Weiss, R. A. *Macromolecules* **1993**, *26*, 6583.
(40) Brozoski, B. A.; Coleman, M. M.; Painter, P. C. *Macromolecules* **1984**, *17*, 230.
(41) O'Connell, E. M.; Root, T. W.; Cooper, S. L. *Macromolecules* **1994**, *27*, 5803.

MA951441J